

REACTION BETWEEN CO₂ AND COKE DOPED WITH NaCN

M. ALAM and T. DEBROY

Department of Materials Science and Engineering, The Pennsylvania State University,
University Park, PA 16802

(Received 18 September 1986; in revised form 24 October 1986)

Abstract—The role of NaCN as a catalytic precursor in the reaction between coke and carbon dioxide is examined. The experimental work included determination of reaction rate, examination of the chemical stability of NaCN and characterization of coke at various stages of reaction. The extent of sodium-carbon contact was physically modelled by examining the distribution of potassium in the interior of a KCN doped coke sample after partial reaction.

Physical evidence is presented to demonstrate that at 1123 K, the vapor cycle mechanism is the predominant mode of catalysis with catalyst concentration and specific surface area being the two most important directly measureable rate determining factors. Analysis of the rate data on the basis of a structural model demonstrated that when NaCN was used, the enhancement of the rate was inadequate for the diffusion of CO₂ through the porous coke to be important.

Key Words—Gasification, carbon dioxide, sodium cyanide, coke

1. INTRODUCTION

The reaction between coke and carbon dioxide commonly known as the Boudouard reaction has been the subject of extensive research in the last several decades and several reviews are now available on this topic[1-4]. The large and proliferating literature on the reaction:



is a testimony of both the importance and the complexity of the reaction. The importance of this reaction originates from the occurrence of this reaction in a number of metallurgical and chemical reactors. The complexity arises from the frequent involvement of many factors that influence the reaction rate. A large number of factors such as the crystallinity of carbon, concentration of active sites on the coke surface, the pore structure of coke and the nature and concentration of inorganic impurities influence the rate of the coke-carbon dioxide reaction[4]. Among the inorganic compounds, several alkali metal salts[5-11] are of particular importance since these are either easily converted to an elemental form or transformed to compounds that are intermediate products in the gasification of carbon.

In a number of metallurgical and chemical reactors, sodium cyanide[12] is formed in the high temperature region of the furnace. Although several sodium salts are known to be highly active precursors in the catalysis of reaction (1), the role of NaCN has not been investigated. In the absence of a catalyst in coke, the rate of diffusion of CO₂ through the gas boundary layer and the porous coke is often faster than the rate of the intrinsic chemical reaction between coke and CO₂[13]. However, when a catalyst

is added to the coke, the rate of the chemical reaction is dramatically enhanced. Thus the diffusion processes become relatively more important and the role of structural parameters becomes vital in determining the rate of the reaction.

The primary objective of this work is to investigate the structural effects in the reaction between carbon dioxide and coke doped with various amounts of NaCN. The changes in the specific surface area of coke due to reaction were determined by nitrogen adsorption technique. The pore structure was examined by mercury porosimetry and scanning electron microscopy. The changes in the concentration of sodium were studied by atomic absorption technique. The catalyst-carbon contact was investigated by doping a few coke samples with KCN and examining the distribution of K by energy dispersion X-ray studies. The "modeling" was necessary since it is difficult to determine the distribution of Na in the coke structure. The catalytic effect of NaCN is compared with that of KCN. Furthermore, since sulfur is known to influence the coke-CO₂ reaction[14], the changes in the concentration of sulfur due to the reaction were also investigated.

The rate of reaction between CO₂ and coke doped with various concentrations of NaCN was determined by thermogravimetry. The rate data were analyzed to examine the influences of the structural parameters. The contribution of pore diffusion in the overall rate was calculated by using a mathematical model with due considerations to the structural changes.

2. EXPERIMENTAL

2.1 Sample preparation

The proximate and ultimate analyses and the ash composition of the coke are given in Table 1. The

Table 1. Proximate and ultimate analyses and ash composition of experimental coke

<i>Proximate Analysis</i>	
Fixed Carbon	93.47%
Volatiles	2.01%
Moisture	0.28%
Ash	5.52%
<i>Ultimate Analysis (dry basis)</i>	
Carbon	92.10%
Hydrogen	0.23%
Nitrogen	1.30%
Sulfur	0.61%
<i>Ash Composition</i>	
SiO ₂	53.2%
Al ₂ O ₃	22.3%
Fe ₂ O ₃	14.4%
TiO ₂	2.68%
K ₂ O	1.71%
MgO	0.83%
CaO	0.7%
Na ₂ O	0.08%
Cr ₂ O ₃	0.07%

coke had a reactivity of 17.1% on the Bethlehem scale[15]. The coke was pulverized and the fraction -270 + 325 mesh was thoroughly mixed with NaCN using a pestle and mortar and discs of 9.5×10^{-3} m diameter and 4.75×10^{-3} m thickness were then pressed under a 3.52×10^5 kg load. A small amount of deionized water was used as a binder. The bulk density of the pellets was about 1.5×10^3 kg/m³.

2.2 Thermogravimetry

The thermogravimetric set-up used is shown schematically in Fig. 1. It consisted of a Cahn microbalance (Model 1000, 0.5 microgram sensitivity) and a high temperature silicon carbide vertical tube furnace with a 0.025 m long equitemperature zone at the center. The temperature was regulated by a Eurotherm controller to an accuracy of ± 2 K. The gas purification train had provisions for the removal of moisture, hydrocarbons, O₂, CO and CO₂.

The coke pellet was placed in a platinum wire basket and was suspended from one arm of the Cahn balance with a .0005 m diameter platinum wire. The system was first purged with argon flowing at a rate of 8.3×10^{-6} m³/s at 298 K and 101.3 kPa total pressure for 1800 s. The furnace was then heated to 473 K for the removal of moisture from the sample. After moisture removal, indicated by a constant sample weight on a strip chart recorder, the furnace temperature was raised to the reaction temperature (1123 K). The furnace heating rate was kept constant for all the runs. After reaching the desired temperature, the flow rates of the reacting gases were adjusted to the required values.

2.3 Identification of the sodium compounds and determination of the concentration of sodium

A Rigaku X-ray Diffractometer was used for identification of the sodium salts in the partially reacted

coke samples. A Perkin Elmer Model 703 Atomic Absorption Spectrometer was used to determine the changes in the concentration of sodium in the coke samples.

2.4 Characterization of coke structure

The structure of the coke samples was characterized with regard to specific surface area, pore size distribution, porosity and mean pore radius.

The specific surface area of the coke was determined by nitrogen adsorption and the BET treatment of the adsorption isotherms. A Quantasorb Sorption System was used with He as the carrier gas.

The pore size distribution, porosity and average pore radius of the coke were determined by mercury intrusion technique using an Aminco (1.034×10^5 kPa) digital read out porosimeter. The porosimeter had a capability to determine the equivalent pore radius from 50 to 0.007 μ m (assuming 130° contact angle).

The microstructural changes of the coke samples were examined by Scanning Electron Microscopy.

3. RESULTS AND DISCUSSION

3.1 Chemical stability of NaCN

Sodium cyanide added to the coke may react with CO₂ during coke gasification. The following reactions can occur.

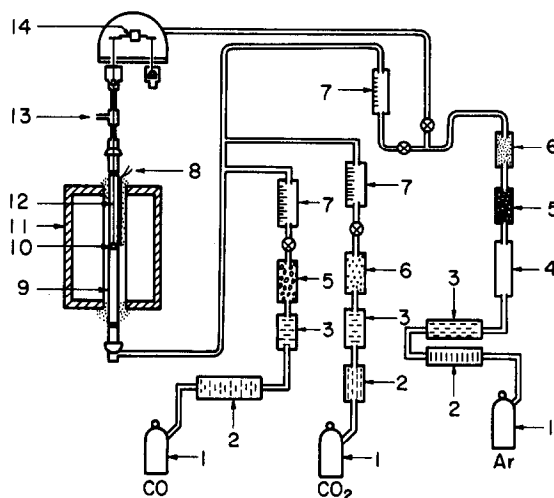
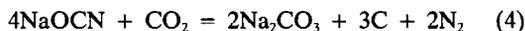
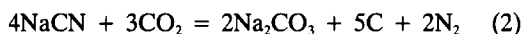


Fig. 1. Schematic diagram of the experimental set-up. 1) Gas cylinder 2) Drierite Column 3) Activated charcoal column 4) Titanium chips 5) Ascarite column 6) Activated alumina column 7) Rotameter 8) Control thermocouple 9) Mullite reaction tube 10) Coke pellet 11) Furnace shell 12) Platinum suspension wire 13) Gas outlet 14) Cahn balance.

Table 2. Phase identification ($T = 1123$ K, $P_{\text{CO}_2} = 101.3$ kPa)

Catalyst	$W \times 10^6$ (kg)	$\frac{\text{kg mole Na}}{\text{kg mole C}}$	Burn Off (F)	Phases Identified	Match*
NaCN	483.8	0.065	0.205	NaCN	3/4
				NaOCN	5/10
				Na ₂ CO ₃	11/18
NaOCN	465.7	0.049	0.209	NaOCN	5/10
				Na ₂ CO ₃	9/18

*Number of peaks observed/number of peaks listed in powder diffraction file.

To examine the reaction between NaCN present in coke and CO₂, a sample containing coke and NaCN was reacted with pure CO₂ until 20% of the initial sample weight was lost. The sample was then analyzed by X-rays to detect the sodium compounds. The results are presented in Table 2 which indicates that NaCN in the coke reacted with CO₂ to form NaOCN and Na₂CO₃. A sample containing coke and NaOCN was also reacted with pure CO₂ to examine the feasibility of reaction (4). The partially reacted sample was then analyzed by X-rays and the results are presented in Table 2. The data indicate that NaOCN indeed react with CO₂ to form Na₂CO₃.

3.2 Decay in the concentration of sodium

In an earlier study[16] in our laboratory it was found that molten NaCN vaporizes at fairly high rates at temperatures above 900 K. It is also known that when sodium salts are added to carbon, sodium vapor is formed during the catalytic gasification process.

Several experiments were conducted to determine the extent of sodium loss during gasification of coke containing NaCN. In each case, a coke sample containing NaCN (kg mole Na/kg mole C = 0.005) was gasified in pure CO₂ at 1123 K to different degrees

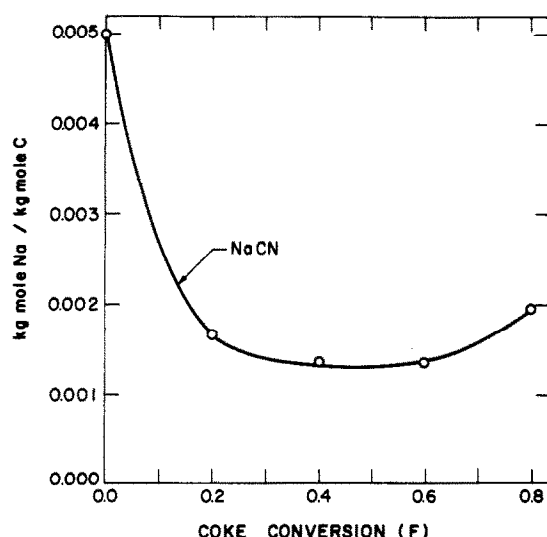


Fig. 2. Sodium concentration changes during reaction. ($T = 1123$ K, $P_{\text{CO}_2} = 101.3$ kPa, initial kg mole Na/kg mole C = 0.005).

of coke conversion in the range of 0–80% of the initial weight of the sample. The partially reacted samples were then analyzed for total sodium by atomic absorption spectroscopy. The results are presented in Fig. 2 as kg mole Na/kg mole C ratios measured at various conversions. The decrease of the molar ratio in the initial period is indicative of a relatively higher rate of loss of sodium than the rate of carbon gasification. The sodium may be lost from the coke pellet as NaCN. With the progress of the reaction, NaCN is converted to other less volatile compounds. Subsequently, the rate of loss of sodium decreases as compared to the carbon gasification. This results in an increase in the kg mole Na/kg mole C ratio with the progress of the reaction.

3.3 Variation of specific surface area

Surface area measurements were carried out on several partially reacted coke samples with or without the addition of NaCN. The added concentration of NaCN in each case corresponded to kg mole Na/kg mole C ratio of 0.005. The specific surface

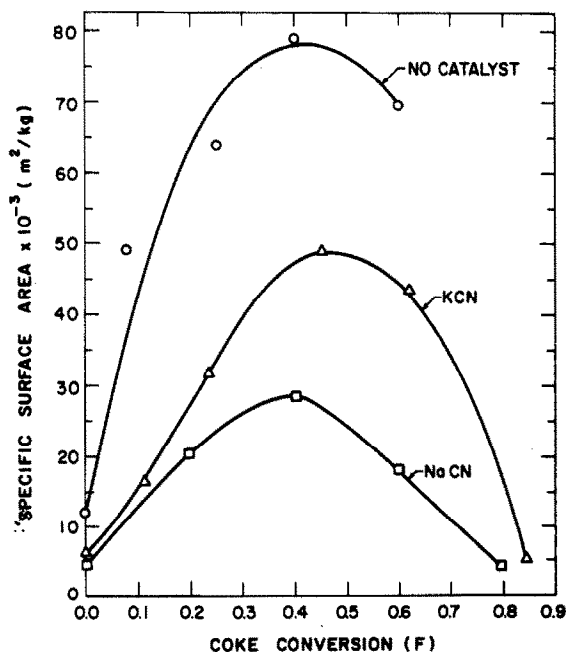


Fig. 3. Specific surface area changes during reaction. ($T = 1123$ K, $P_{\text{CO}_2} = 101.3$ kPa, initial kg mole M/kg mole C = 0.005. M = Na or K).

area changes for the noncatalyzed and for the catalyzed CO_2 gasification of coke as a function of coke conversion are shown in Fig. 3. The data indicate that, the specific surface area of coke samples with and without the presence of NaCN increases with conversion initially, reaches a maximum and decreases towards the end. The data in Fig. 3 also indicate that the specific surface areas of coke samples doped with NaCN are significantly lower than the surface area for the coke sample containing no NaCN. Shadman and co-workers[17] observed a similar behavior in the KOH catalyzed CO_2 gasification of coal char and attributed the decrease in the specific surface area to catalyst induced pore plugging. Since addition of NaCN reduces the specific surface area, the influence of the concentration of NaCN on the specific surface area was examined. The coke samples were impregnated with various concentrations of NaCN and then heated in an atmosphere of argon until a temperature of 1123 K was reached. At this stage, the heating was terminated, the specimens were cooled and their specific surface area was measured. The results are presented in Fig. 4 as specific surface area vs. kg mole Na/kg mole C ratio plot. The figure indicates that the addition of a small quantity of NaCN reduces the specific surface area significantly. Since molten NaCN vaporizes at a significant rate at the reaction temperature, the interior of the pores are well covered by the alkali. This extensive surface coverage seems to reduce the specific surface area. However, when the concentration of NaCN in coke is relatively high, further addition of NaCN has a relatively small effect on the specific surface area. This is due to the fact that at higher concentrations of NaCN, the amount of surface available for gas adsorption be-

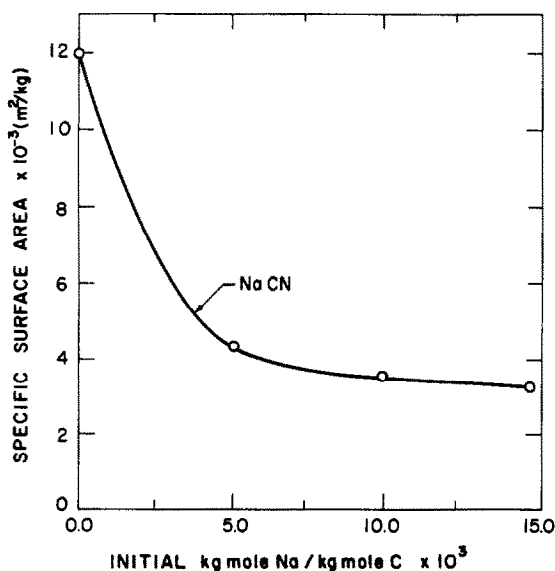


Fig. 4. Specific surface area as a function of initial kg mole Na/kg mole C. ($T = 1123$ K, $P_{Ar} = 101.3$ kPa, $F = 0.0$).

comes rather small and further addition of NaCN has only a marginal effect on the surface area.

In an earlier study[18] we found that the manner in which the specific surface area changed with conversion was not significantly affected by the anionic component of various potassium bearing precursors. To examine the effects of the cationic component of cyanides we measured the specific surface area of coke samples doped with KCN as a function of conversion. The measured values are presented in Fig. 3 along with the data for NaCN. The figure indicates that addition of NaCN to coke results in a more significant decrease in surface area of coke as compared to KCN addition. This observation is consistent with the relatively higher vapor pressure and lower melting temperature of NaCN as compared to KCN[19].

The effects of the degree of conversion and the concentration of NaCN on the specific surface area can be explained by our data on electron microscopy and pore size distribution studies on various partially reacted samples.

3.4 Variation of pore size distribution

Pore size distribution was studied by measuring the extent of mercury penetration in cm^3/gm as a function of applied pressure. The coke samples used were impregnated with NaCN at a concentration corresponding to kg mole Na/kg mole C ratio of 0.005 and reacted to various degrees. The percentage of the total pore volume contributed by all pores having a radius larger than r_p is plotted against the minimum pore radius, r_p , in Fig. 5. The data in this figure indicate that % pore volume contributed by pores of radius $0.1 \mu\text{m}$ or larger increases with coke conversion in the initial period of reaction. This observation is also true for pores of $1.0 \mu\text{m}$ or larger. However, when large pores ($>10 \mu\text{m}$) are considered, the percentage volume contributed by these pores decreases with increasing conversion up to 40% conversion. Thus, up to 40% conversion, small pores are generated with the progress of the reaction. Beyond 40% conversion, small pores are enlarged and this accounts for the decrease in the specific surface area.

Microstructures of the fractured surfaces of various partially reacted coke samples are also consistent with the results of pore size distribution studies by mercury porosimetry. A comparison of the micrographs of unreacted coke and coke after 20% reaction indicated that in the early stages of reaction some new small pores are generated. This is consistent with the results of mercury porosimetry and also with the observed increase in the specific surface area with conversion at the initiation of the reaction. At 60% conversion relatively large pores were observed in the microstructure. This, again is consistent with the decrease in the specific surface area at high conversions observed from nitrogen adsorption measurements.

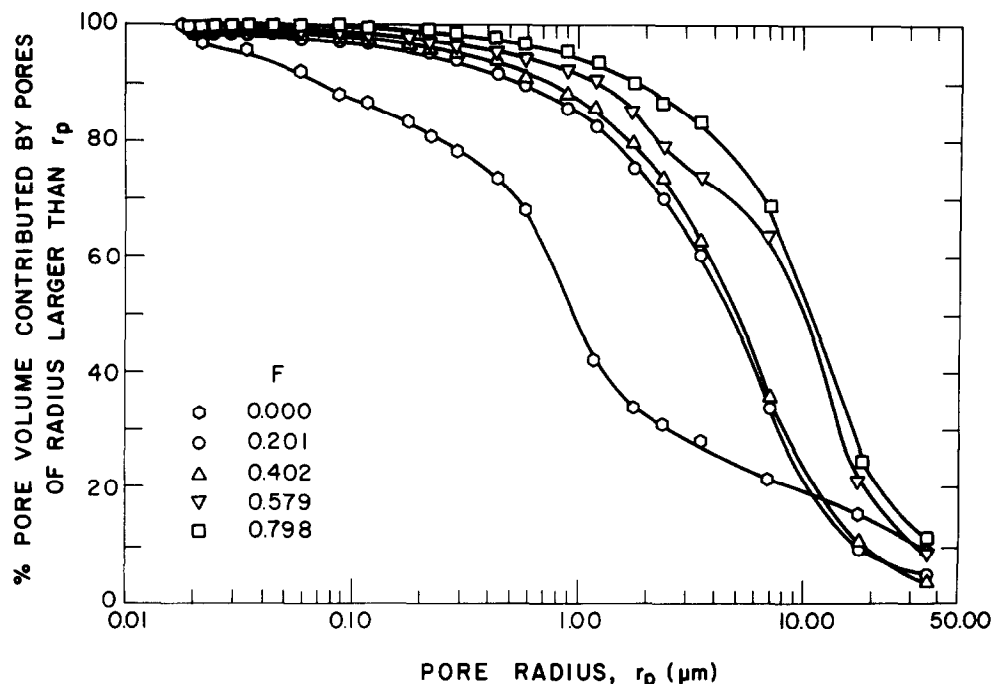


Fig. 5. Percent pore volume contributed by pores of radius larger than r_p vs pore radius, r_p , plots for NaCN doped samples. ($T = 1123$ K, $P_{\text{CO}_2} = 101.3$ kPa, initial kg mole Na/kg mole C = 0.005).

3.5 Variation of sulfur concentration with conversion

Since sulfur may influence the rate of coke-CO₂ reaction, the concentration of sulfur in the coke was determined as a function of the extent of conversion. The data on the concentration of sulfur are presented in Table 3 for coke samples with or without the addition of NaCN. It may be observed from the data that the concentration of sulfur did not change significantly with the extent of reaction in both catalyzed and noncatalyzed runs. Therefore, the effect of sulfur in noncatalyzed reaction was not significantly different from its effects in catalyzed runs. Furthermore, the effect of sulfur was fairly constant during the reaction of coke for both catalytic and noncatalytic reactions. The difference in the reaction rates between samples with and without the additions of catalytic precursors can be attributed to the true effects of the precursors and not to unequal changes in the sulfur concentrations in the two cases.

3.6 Reaction kinetics

3.6.1 Catalytic effects. The rate data for the reaction between coke samples and CO₂ with and without the presence of NaCN are presented in Fig. 6 in the form of fractional weight loss, F , vs. reaction time, t , plots. The fractional weight loss, F , sometimes referred to as coke conversion is defined as:

$$F = \Delta W / W_0 \quad (5)$$

where ΔW is the weight loss sustained by the sample

and W_0 is the initial weight of the coke pellet. Since the addition of NaCN enhances the rate of coke-CO₂ reaction, the rate of reaction is not controlled solely by the physical diffusion of gases through the coke structure and through the gas boundary layer. A quantitative assessment of the contribution of the transport steps in the reaction rate is deferred until the end of this section.

Earlier work in our laboratory[18] has established that when coke is doped with several catalytic precursors containing potassium, the catalytic effects were practically independent of the anionic constituents of the precursors. In the current study, the cationic constituent of the dopant, i.e., Na was replaced in some experiments by K to compare the relative catalytic effects of KCN and NaCN. These experiments had two specific objectives. First, the use of KCN allowed us to examine the distribution of K in the partially reacted specimens and the results provided insight about the extent of precursor-car-

Table 3. Sulfur contents of partially reacted coke samples with and without the presence of NaCN. ($T = 1123$ K, $P_{\text{CO}_2} = 101.3$ kPa, initial kg mole Na/kg mole C = 0.005)

Conversion, F	Wt% S	
	Catalyzed	Non-catalyzed
0.0	0.56	0.61
0.2	0.61	0.58
0.6	0.58	0.69

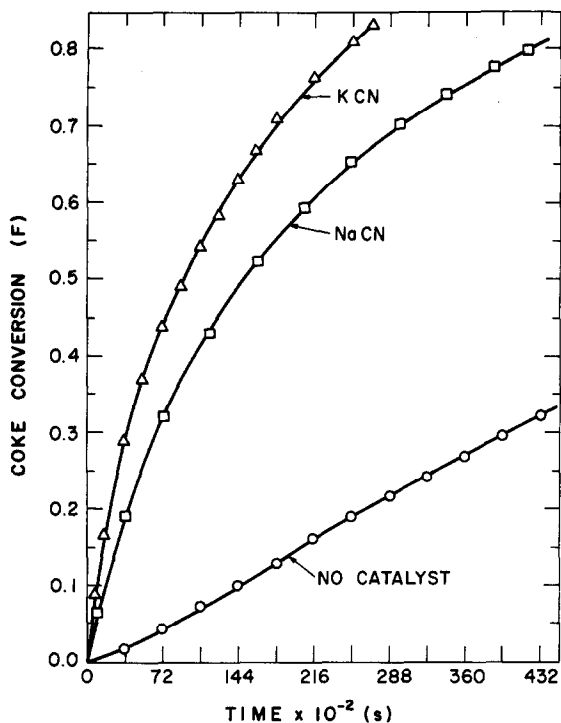


Fig. 6. Coke conversion as a function of time. ($T = 1123$ K, $P_{\text{CO}_2} = 101.3$ kPa, initial kg mole M/kg mole C = 0.005. M = Na or K).

bon contact. The distribution of K was determined by the X-ray energy dispersion studies. Since the distribution of Na in the coke pellet cannot be easily determined by X-ray studies, the studies provide useful qualitative information of the anticipated Na distribution in the coke pellet. Secondly, the use of KCN as a catalytic precursor was also useful for the examination of the effects of variation of the cationic

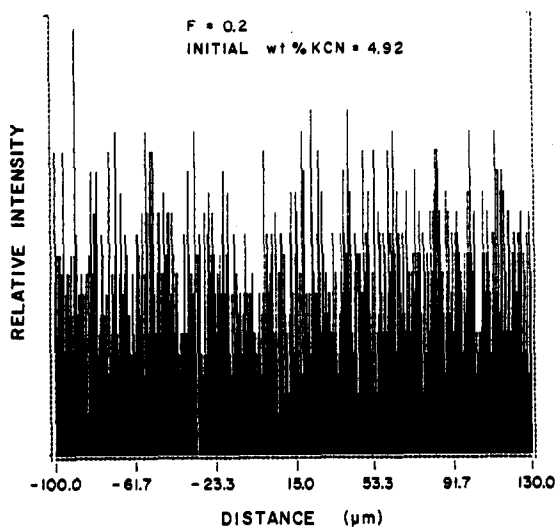
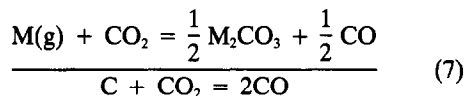
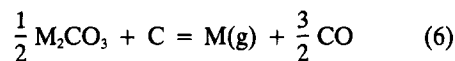


Fig. 7. Potassium distribution along a fractured surface of coke pellet. ($T = 1123$ K, $P_{\text{CO}_2} = 101.3$ kPa). (Ref. 18)

constituents Na^+ and K^+ of the precursors keeping the anionic constituent (CN^-) as a constant. To examine the carbon-precursor contact, a coke sample doped with 4.92 wt% KCN was gasified to 20% in pure CO_2 at 1123 K and the distribution of K was examined in the interior of the coke pellet. A typical distribution pattern for potassium is shown in Fig. 7. The data indicate that practically the entire area is covered by potassium. Such an extensive coverage cannot occur by the spreading of a melt in the interior of the fine pores. Potassium must have transported via gas phase either in elemental form or as a volatile compound. It may be of interest to note that if the transport of cyanide vapors is a major contributing factor in the distribution of alkali metals, the surface coverage of sodium will be as extensive as that of potassium since sodium cyanide vaporizes at a higher rate than potassium cyanide under identical conditions.

The influence of NaCN and KCN on the enhancement of the rate of CO_2 gasification of coke is presented in Fig. 6. The data indicates that KCN enhances the rate more than NaCN. This observation can be explained on the basis of the vapor cycle mechanism[7]. The steps involved in the mechanistic scheme can be represented by the following chemical reactions:



where M is either Na or K. Following the generation of M_2CO_3 by reactions (2)–(4) the catalysis can proceed via reactions (6) and (7). The presence of an adequate amount of metal vapor is central to the catalytic process. Therefore, in reaction (6) the equilibrium partial pressures of Na and K vapors can give some idea about the relative effectiveness of NaCN and KCN as catalytic precursors. From the available thermodynamic data[19], the equilibrium pressures of Na(g) and K(g) were calculated at several P_{CO} values for the experimental conditions and the results are presented in Table 4. The data indi-

Table 4. Equilibrium pressures of Na(g) and K(g) at 1123 K and different P_{CO} values

P_{CO} (kPa)	$P \times 10^2$ (kPa) calculated from reaction (6)	
	Na	K
10.13	6.96	17.51
20.26	2.49	6.19
40.52	0.88	2.19
60.78	0.48	1.20
81.04	0.31	0.77
91.17	0.26	0.65

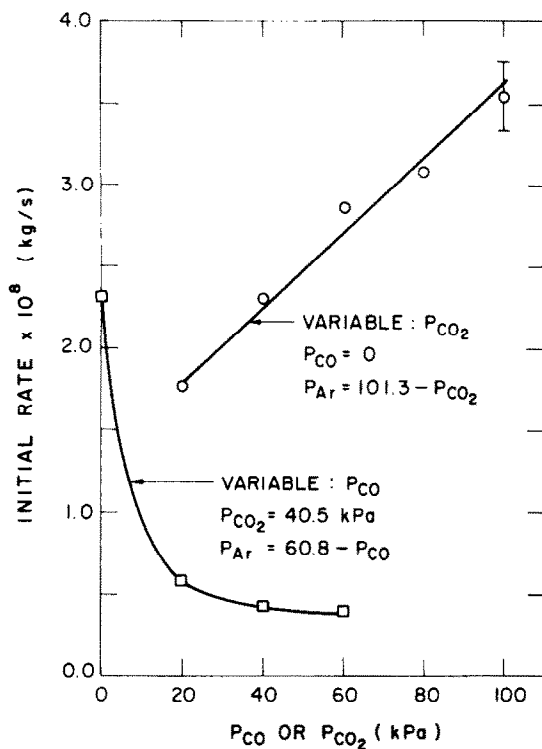


Fig. 8. Effects of the partial pressures of CO and CO₂ on the rate of coke-CO₂ reaction in the presence of NaCN. ($T = 1123 \text{ K}$, initial kg mole Na/kg mole C = 0.005).

cate that the equilibrium partial pressure of K is higher than that of Na. The calculated vapor pressures of Na and K are therefore consistent with the relative catalytic effects of NaCN and KCN observed in Fig. 6.

Reaction rate measurements were also carried out in various partial pressures of CO and CO₂ to examine if the influence of the partial pressures of these gases on the reaction rate can be explained on the basis of the above mechanistic scheme. The rate data are presented in Fig. 8. The figure indicates that addition of CO significantly retards the rate of coke-CO₂ reaction in presence of NaCN. Also the partial pressure of CO₂ influences the reaction rate. These observations are in agreement with the importance of reactions 6, 2 and 4 in determining the overall rate.

3.7 Effect of sodium concentration changes and specific surface area changes

Unless the diffusion of CO and CO₂ through the pore structure of coke is slower than the rate of reaction of CO₂ both the specific surface area of the coke and the catalyst concentration should have appreciable effect on the rate of reaction. In Fig. 9, the rate of reaction per unit surface area of coke samples, with or without the addition of NaCN, is plotted as a function of conversion. By decoupling the rate data from the effects of surface area changes, the effects of sodium concentration changes on the

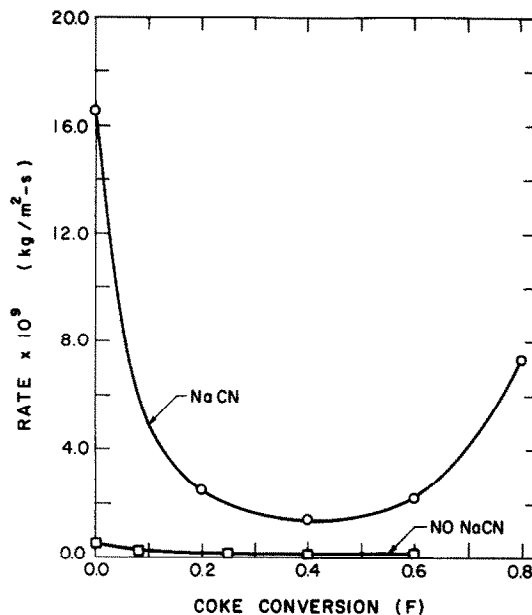


Fig. 9. Rate per unit surface area vs. coke conversion. ($T = 1123 \text{ K}$, $P_{CO_2} = 101.3 \text{ kPa}$, initial kg mole Na/kg mole C = 0.005).

reaction rate can be enhanced. For the sample without NaCN addition, the rate per unit surface area remains almost constant up to 60% conversion. For the coke sample doped with NaCN, the rate per unit surface area decreases initially with conversion, remains fairly constant up to about $F = 0.6$ and then increases. The shape of this plot resembles the shape of the kg mole Na/kg mole C ratio vs. time plot presented earlier in Fig. 2. Therefore, it seems that once the geometrical effect of the surface area changes are eliminated from the rate data, the variation in reaction rate appears to be similar in nature to the variation in the concentration of sodium. In fact, when the initial rates of samples doped with various concentrations of sodium are plotted as a function of the concentration of sodium, and the structural effects are eliminated to a large extent, the rate seems to be proportional to the concentration of sodium (Fig. 10).

Again, the rate data can be decoupled from the effects of sodium concentration changes by dividing the rate by the instantaneous concentration of sodium. The reaction rate thus obtained (i.e., based on constant sodium amount), is plotted as a function of the fractional conversion, F in Fig. 11. The trend of the initial increase and the subsequent decay of the reaction rate again, is similar to the changes in the specific surface area presented in Fig. 3. Thus, if the changes in the catalyst concentration are decoupled from the rate data, the influence of the specific surface area on the reaction rate becomes apparent.

The effects of variables other than specific area and the concentration of the sodium can be studied by examining the rate per unit surface area per unit

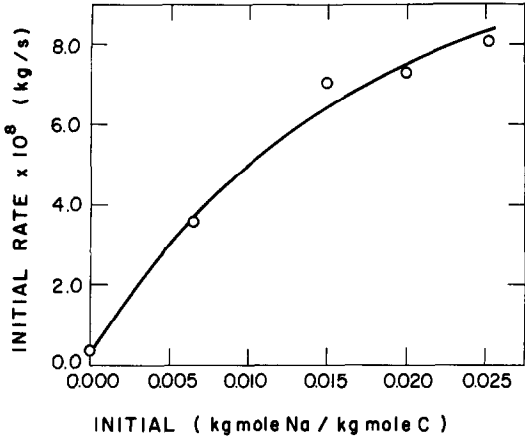


Fig. 10. Initial gasification rate as a function of initial concentration of Na in coke pellet. ($T = 1123 \text{ K}$, $P_{\text{CO}_2} = 101.3 \text{ kPa}$).

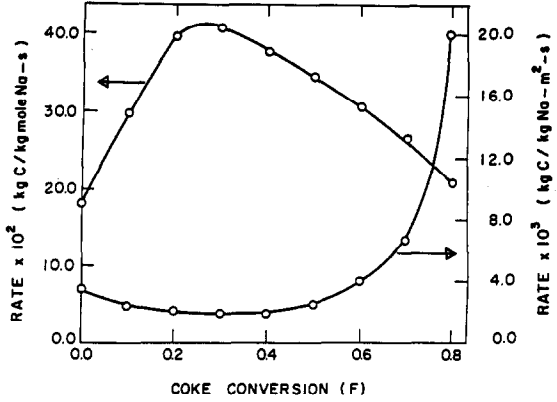


Fig. 11. Rate per unit amount of Na and rate per unit surface area per unit amount of Na vs. coke conversion. ($T = 1123 \text{ K}$, $P_{\text{CO}_2} = 101.3 \text{ kPa}$, initial kg mole Na/kg mole $C = 0.005$).

concentration of the sodium (Fig. 11). The changes in the reaction rate as a function of conversion can be attributed to various other factors including porosity, pore size distribution and the concentration of active sites. Of these factors, the contribution of the pore diffusion in the overall rate can be assessed by examining the values of the effectiveness factor, η , defined as the ratio of the measured reaction rate to the intrinsic reaction rate. The procedure is described below.

3.8 Role of pore diffusion

The effectiveness factor values were calculated following the procedure outlined by Jalan and Rao[6]. The following expression was used for the calculations.

$$\eta = \frac{1}{K_v R T L \left(\frac{1}{K_g} + \frac{L \coth \phi}{\phi D_e} \right)} \quad (8)$$

- where: K_v = intrinsic reaction rate constant in kg mole-s/m²-kg
- R = gas constant = 8314 kg-m²/s²-kg mole-K
- T = temperature in K
- L = characteristic length of the pellet in m
- K_g = gas phase mass transfer coefficient in m/s
- ϕ = dimensionless parameter
- D_e = effective diffusivity of CO₂ in m²/s

The procedure followed for obtaining the values of these variables and the details of the calculation procedure are documented elsewhere[18].

From the knowledge of K_v , L , K_g , D_e and ϕ , the value of the effectiveness factor, η , can be readily determined. It may be of interest to note that since the pore size distribution changes significantly with the reaction time, the value of the effective diffu-

sivity, D_e , must be computed as a function of reaction time. For the calculations reported here, the value of the mean pore size, \bar{r} , was determined from the results of the mercury penetration porosimetry at various coke conversions, using the procedure described by Ritter and Drake[20].

For coke samples doped with NaCN, values of the effectiveness factor, η , are presented in Fig. 12 as a

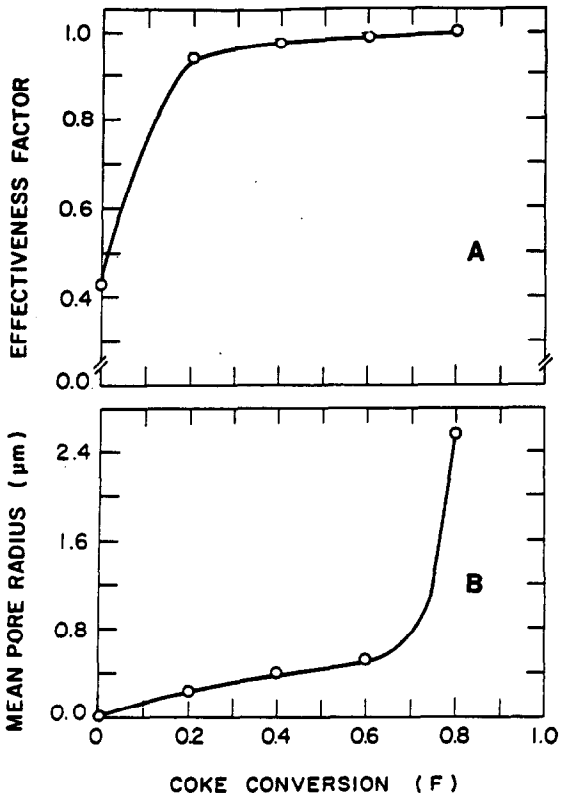


Fig. 12. (A) Effectiveness factor and (B) mean pore radius of NaCN doped samples as a function of coke conversion. ($T = 1123 \text{ K}$, $P_{\text{CO}_2} = 101.3 \text{ kPa}$, initial kg mole Na/kg mole $C = 0.005$).

Table 5. Data for the calculation of effectiveness factor.

Temperature (T): 1123 K
 Partial Pressure of CO₂ in the bulk gas stream (P_b): 1.0133×10^5 kg/m-s²
 Equilibrium pressure of CO₂ (P_e): 0.07×10^5 kg/m-s²
 Pellet diameter (d_p): 9.5×10^{-3} m
 Pellet thickness: (t_p): 4.7×10^{-3} m
 Characteristic length of pellet (L): 1.181×10^{-3} m
 Gas constant (R): 8314 kg-m²/kg mole-s²-K
 Gas phase mass transfer coefficient (K_g): 4.878×10^{-2} m/s
 Binary diffusivity of CO and CO₂ (D_b): 1.516×10^{-4} m²/s

Conversion (F)	Porosity (%) (θ)	Mean pore radius (μ m) (\bar{r})	Rate $\times 10^5$ (kg mole/m ² -s) (J_a)
0.000	37.4	0.015	1.73
0.201	56.4	0.230	1.02
0.402	62.2	0.400	0.61
0.597	70.9	0.500	0.36
0.798	75.2	2.560	0.61

$$\text{Effective diffusivity of CO}_2: D_e = \frac{\theta^2}{\sqrt{3}} D, \text{ m}^2/\text{s}$$

$$\text{Diffusivity of CO}_2 = D = \left(\frac{1}{D_b} + \frac{1}{D_k} \right)^{-1}, \text{ m}^2/\text{s}$$

$$\text{Knudsen diffusivity of CO}_2: D_k = \frac{2}{3} \bar{r} \sqrt{\frac{8RT}{M}} \text{ m}^2/\text{s}$$

function of coke conversion, F . The values of the mean pore radius required for the calculation of the effective diffusivity values obtained from the mercury porosimetry data are also presented in the same diagram. The data for the calculation of η are presented in Table 5. The value of \bar{r} is assumed to be one-third of the average pore radius following the recommendation by Roberts and Satterfield[21]. The computed values of η indicate that at low conversions, when the mean pore size is rather small, the rate of the catalytic reaction is influenced, in part, by the diffusion of CO₂ through the porous coke. However, as the pores are enlarged due to reaction, the pore diffusion is increasingly facilitated and at high conversion values the rate is controlled solely by the chemical reaction.

4. CONCLUSIONS

When coke specimens doped with NaCN are gasified in CO₂, a melt containing Na, C, O and N is formed which on cooling precipitates NaCN, NaOCN and Na₂CO₃. At the reaction temperature, the sodium bearing melt acts as an effective agent for the catalysis of the coke-CO₂ reaction. The concentration of sodium in the coke sample changes significantly with the progress of the reaction.

Model studies using KCN as a dopant revealed extensive coverage of the interior surface of coke by potassium. Such an extensive coverage is possible only if potassium is transported in the interior of the coke via gas phase. This and the analysis of the rate

data are in agreement with the vapor cycle mechanism.

During gasification the initial increase in the surface area is attributed to the generation of small pores, whereas the decrease in the surface area at high conversions is caused by the enlargement of the pores.

Deposition of NaCN in the pores led to a reduction in the specific surface area. The decrease in the specific surface area of coke was less extensive when a relatively lower volatile cyanide, KCN was used as a dopant.

The concentration of sulfur in coke did not change significantly during the reaction. Therefore, the effect of sulfur was fairly constant during the entire period of gasification of coke.

When the effects of the changes of specific surface area and the concentration of sodium were decoupled from the rate, the reaction rate (kg mole C/kg mole Na-m²-s), was found to be relatively insensitive to the extent of the reaction. Thus, changes in specific surface area and the concentration of sodium were the most dominant factors in determining the rate of the catalyzed reaction.

Analysis of the rate data on the basis of a structural model indicates that the enhancement in the gasification rate on addition of NaCN is not sufficient enough for the diffusion of CO₂ through the porous coke to be important.

Acknowledgments—The financial support for this study was provided by the American Iron and Steel Institute under Project No. 34-465.

REFERENCES

1. P. L. Walker, Jr., M. Shelef and R. Anderson, *Chemistry and Physics of Carbon*, (Eds.) P. L. Walker, Jr., Edward Arnold, London, **4**, 381 (1968).
2. J. L. Johnson, *Catal. Rev.* **14**, 1, 131 (1976).
3. W. Y. Wen, *Catal. Rev. Sci. Eng.* **22**, 1 (1980).
4. D. W. McKee, *Chemistry and Physics of Carbon*, (Eds.) P. L. Walker, Jr. and P. A. Thrower, Marcel Dekker, New York, **16**, 1 (1981).
5. M. J. Veera and A. T. Bell, *Fuel* **57**, 194 (1978).
6. Y. K. Rao and B. P. Jalan, *Carbon* **16**, 175 (1978).
7. D. W. McKee and D. Chatterji, *Carbon* **13**, 381 (1975).
8. T. Wigman, A. Hougland, P. Tromp and J. A. Moulijn, *Carbon* **21**, 13 (1983).
9. M. Alam and T. DebRoy, *Met. Trans.* **15B**, 400 (1984).
10. R. T. Hamilton, D. A. Sams and F. Shadman, *Fuel* **62**, 880 (1983).
11. M. Alam and T. DebRoy, *Ironmaking and Steelmaking* **12**, 5, 203 (1985).
12. K. P. Abraham and L. I. Staffansson, *Scand. J. Metall.* **4**, 193 (1975).
13. M. Alam and T. DebRoy, *ISS Trans.* **5**, 7 (1984).
14. K. Otto, L. Bartosiewicz and M. Shelef, *Carbon* **17**, 351 (1979).
15. R. P. Thompson, A. F. Mantione and K. P. Aikman, *Blast Furnace and Steel Plant* **59**, 161 (1971).
16. M. Alam and T. DebRoy, *ISS Trans.* **6**, 15 (1985).
17. D. A. Sams and F. Shadman, *Fuel* **63**, 1008 (1984).
18. M. Alam and T. DebRoy, *Met. Trans.* **17B**, 565 (1986).
19. JANAF Thermochemical Tables, 2nd. Ed., NSRDS-NBS37 (1971).
20. H. L. Ritter and L. C. Drake, *Ind. Eng. Chem. Anal. Ed.* **17**, 12, 782 (1945).
21. G. W. Roberts and C. N. Satterfield, *Ind. Eng. Chem. Fund.* **4**, 288 (1965).